International Journal of Nanomedicine

Dovepress
Taylor & Francis Group

Open Access Full Text Article

ORIGINAL RESEARCH

Injectable Self-Assembling Procyanidin Nanospheres for Effective Osteoarthritis Treatment

Guangjie Li[1,2,*], Fei He[2,*], Jianbao Feng[3], Ge Xu[1], Chengye Wu[1], Yufei Qiao[1], Yang Liu[3], Hanlin Chen[1], Pengcheng Du[4], Jizeng Wang[2]

[1]The First Hospital of Lanzhou University, Lanzhou, Gansu Province, People's Republic of China; [2]College of Civil Engineering and Mechanics, Lanzhou University, Lanzhou, Gansu Province, People's Republic of China; [3]Hospital of Stomatology, Lanzhou University, Lanzhou, Gansu Province, People's Republic of China; [4]College of Chemistry and Chemical Engineering, Lanzhou University, Gansu Province, People's Republic of China

*These authors contributed equally to this work

Correspondence: Jizeng Wang, Email jzwang@lzu.edu.cn

Background: Osteoarthritis (OA), a prevalent joint disease, causes immense suffering to thousands of patients, impairing their mobility and diminishing their quality of life. Current treatment methods primarily rely on analgesics or anti-inflammatory drugs to alleviate symptoms but fail to achieve the desired therapeutic outcome.

Methods: To better realize therapeutic effects of OA, procyanidins (PAs), as a type of plant flavonoids with strong antioxidant and anti-inflammatory activities, were designed to self-assembly with well-dispersible Pluronic F127 (PF127) through the hydrogen-bond interaction to present an injectable, biocompatibility PA nanospheres.

Results: These nanospheres significantly increased the cell viability in mouse L929 fibroblasts and ADTC5 chondrocytes compared with unassembled PAs. In addition, the self-assembling PAs/PF127 nanospheres enhanced the protein expression of collagen (COL1A1 and COL3A1) in fibroblasts, and the expression of glycosaminoglycan and COL2A1 was also higher than unassembled PAs in chondrocytes, this heralded the potential to achieve OA repair strategies at the cellular level. In an enzymolysis model of rat OA, PAs/PF127 nanospheres significantly reduce joint space swelling in the early stages of cartilage destruction and accelerate the formation of subchondral bone and cartilaginous surface.

Implication: This study offers valuable insights into the preparation of novel PA nanospheres for effective repair of OA.

Keywords: procyanidin, self-assembling nanospheres, injectable, osteoarthritis treatment

Introduction

Osteoarthritis (OA) is a degenerative disease characterized by the progressive loss of joint cartilage, which is one of the main causes of disability worldwide.[1–4] The pathogenesis of OA is complex and involves biomechanical, genetic, and hormonal factors that play important roles in its occurrence and development.[5] Cartilage damage cannot naturally heal due to poor blood supply, and the destruction of cartilage structure leads to biomechanical changes in joints, accelerating the progression of OA.[6] Therefore, actively repairing cartilage damage is important in improving the prognosis of osteoarthritis. Currently, there are various treatments available for OA, including acupuncture therapy, drug treatment and surgical therapy.[7,8] Painkillers and anti-inflammatory drugs are commonly used for OA, but they only alleviate symptoms and do not provide a cure. Surgical interventions such as subchondral bone microfracture, lavage, debridement, and shaving are effective for small chondral defects but are not suitable for severe articular lesions.[9] Autologous or allogenic cartilage grafts can be used to treat severe lesions, but they may cause complications at the donor site. Total joint arthroplasty is an effective treatment for OA, but open surgery has a large traumatic impact and is not acceptable for most mild patients. Therefore, early-stage therapeutic interventions for OA can prevent disease aggravation and are more

Received: 11 October 2024
Accepted: 22 January 2025
Published: 29 January 2025

conducive to patient treatment and relief. Therefore, it is essential to develop new strategies for repairing cartilage damage in OA patients.

Nonsteroidal anti-inflammatory drugs (NSAIDs), specific cyclooxygenase (COX)-2 inhibitors, and opioids are commonly used for early treatment of OA. While NSAIDs have good analgesic effects, intra-articular injection drugs face the problem of fast clearance in synovial fluid and short retention time.[10,11] Furthermore, chronic and frequent local injection of glucocorticoids can lead to osteoporosis, infections, and even cartilage loss.[12] In addition, intra-articular injection prolongs the therapy cycle, which decreases patient compliance to some extent. Therefore, drug treatment for early OA should focus on ensuring steadily released medication with clarified therapeutic effects on damaged cartilage and ligaments. However, commonly used intra-articular injectable agents, including both small molecular and macromolecular drugs, suffer from rapid clearance of synovial fluid and short retention time. Platelet-rich plasma (PRP) and mesenchymal stem cells (MSCs) have been injected into joint cavities for OA treatment, but only a few cells survive or remain in situ. Consequently, developing an innovative non-surgical technique to achieve improved lubrication and local drug delivery is highly desirable for maintaining healthy joints. This would also be highly meaningful in reducing cartilage wear and relieving inflammatory symptoms in OA treatment.

Injectable materials, including hydrogels and hydrogel microspheres, have been extensively researched for their potential use in intra-articular injections to treat OA, which is attributed to their minimally invasive manner, extended drug retention time and high loading efficiency.[13,14] Hyaluronic acid (HA) is a commonly used substance in OA treatment, where it is injected into the joints to provide lubrication. This can absorb and distribute the impact forces caused by movement and pressure, thereby reducing joint pain and inflammation. Cross-linked HA hydrogel has been shown to have a longer retention time in the body, leading to improved cartilage cell density and matrix appearance.[15] Additionally, incorporating anti-inflammatory agents such as Dexamethasone (Dex) and Sodium Diclofenac (DS) into hydrogel microspheres allows for controlled drug release, prolonging drug retention in the joints while minimizing adverse effects.[15–17]

Recently, natural products have been evaluated for their potential role in the prevention and treatment of OA. These products offer a safe and effective adjunctive therapeutic approach, such as turmeric, thymoquinone, epigallocatechin 3-gallate (EGCG), and others that have been well documented to have beneficial effects against arthritis.[18–20] However, despite their promising results, natural product extracts face challenges such as low bioavailability, short retention time, and potential side effects during treatment. To address these issues, researchers have explored incorporating these drugs into hydrogels or microspheres, which can lead to improved efficacy in the treatment of OA.[21,22]

In this study, we construct an injectable, biocompatible, and self-assembling PA nanospheres (PAs/PF127), which is formed using a self-assembly strategy based on PF127 and PAs through hydrogen-bond interactions. Our results demonstrate that these nanospheres significantly improve the cell viability in mouse L929 fibroblasts and ADTC5 chondrocytes. Furthermore, PAs/PF127 nanospheres enhance collagen protein expression (COL1A1 and COL3A1) in fibroblasts and increase glycosaminoglycan abundance in chondrocytes, suggesting their potential for OA repair strategies. In an enzymolysis model of rat OA, PAs/PF127 nanospheres significantly reduce joint space swelling in the early stages of cartilage destruction and accelerate subchondral bone and cartilaginous surface formation. This novel nanosphere formulation is easy to prepare and has promising applications for cartilage healing, with significant implications for the field of OA repair.

Experimental Section

Materials

Pluronic F127 (PF127) was received from Sigma-Aldrich. Procyanidins (PAs) were purchased from Macklin Co., Ltd. (Shanghai, China). Dimethyl sulfoxide (DMSO) was obtained from Sinopharm Chemical Reagent Co. Ltd. The dialysis bag with the molecular weight cutoff (MWCO) of 3500 was obtained from Shanghai Yuanye Bio-Technology Co. Ltd. Distilled water was used throughout the experiment.

Preparation of Procyanidins-PF127 (PAs/PF127) Self-Assembled Nanospheres

As shown in Figure 1A, the PAs/PF127 self-assembled nanospheres are prepared using hydrogen bond interaction between procyanidin and PF127. Generally, 50 mg of PF127 and PAs (10, 25, 50, 75, 100 mg) were dissolved in 5 mL of DMSO at room temperature, and the ratio of each component was listed in Table 1. After stirring for 1 h, the mixed solution was transferred into a dialysis bag with a MWCO 3500 Da, then dialyzed against DI-water at room temperature for 48 h. The PAs/PF127 samples were obtained by freeze-drying.

Characterization

Transmission electron microscopy (TEM) analysis was used to characterize the morphology of nanospheres by JEM-2100 transmission electron microscopy (JEOL, Japan). Dynamic light scattering (DLS) and Zeta potential measurements were investigated with the 90Plus Pals equipment at 25 °C (Brookhaven Instruments Corporation, USA). The scattering intensities of the samples were measured at a 90° angle using a photomultiplier tube. Fourier transform infrared spectroscopy (FT-IR) spectral analysis was analyzed from 4000 to 400 cm^{-1} using the Thermo Fisher Nicolet is5 infrared spectrometer (Bruker, Karlsruhe, Germany).

Cumulative Release of Procyanidin From PAs/PF127

The release behavior of PAs/PF127 was evaluated by dispersing an exact amount of PAs/PF127 in 5 mL of pH 7.4 PBS and simulating normal physiological conditions. The solution was then transferred into a dialysis bag (MWCO: 8000–14,000 Da) and immersed in 100 mL of the corresponding buffer solution. The release process was conducted at 37 °C in an incubator shaker over varying time intervals. At designated time points, a fixed volume of the dialysate was collected for UV-Vis analysis, and an equal volume of fresh buffer solution was added to maintain a constant volume.

Cell Culture

Mouse L929 fibroblasts and ADTC5 chondrocytes were used to evaluate the cell response for PAs/PF127. Both cells were purchased from the Cell Bank of the Chinese Academy of Sciences (Shanghai, China). L929 fibroblasts were cultured in DMEM with 10% horse serum (Solarbio, Beijing, China) and 1% penicillin/streptomycin solution (Solarbio, Beijing, China). ADTC5 chondrocytes were cultured in DMEM with 10% fetal bovine serum (FBS, GibcoTM, USA) and 1% penicillin/streptomycin solution, and all cells were cultured in a humidified atmosphere at 37 °C, 5% CO_2. The fresh medium was replaced once every two days. Cells were trypsinized using 0.25% trypsin/EDTA (Solarbio, Beijing, China) and passaged after reaching 80% confluence and subcultured at the density of 5000 cells cm^{-2}.

Cell Viability

To verify the biocompatibility of PAs/PF127 nanospheres, CCK-8 method and live/dead viability staining (L7012, Thermo Fisher, Waltham) were performed to assess the cell viability of mouse L929 fibroblasts and ADTC5 chondrocytes. Specifically, after being sterilized by ethylene oxide (disinfection supply room, the First Hospital of Lanzhou University), freeze-dried PAs/PF127 were resolubilized in DMEM (0.1 g/50 mL). Both types of cells (2×10^4 cells/well in a 6-well plate) were cultured in 0%–20% PAs/PF127-DMEM supplied serum and antibiotic, respectively. After culturing for 4 days, the cells were washed with DPBS (Solarbio, Beijing, China) for three times and incubated with CCK-8 reagent for 2 hours according to the manufacturer's instructions, six parallel holes were set for each group, and the 450 nm absorbance was measured by a microplate reader (Mode-680, Bio-Rad).

Furthermore, the cultures were stained with L7012 according to manufacturer's protocol, and the stained cells were visualized using a fluorescence microscope (BX53, Olympus, Japan). Red under the microscope represented dead cells and green showed the live cells.

Elisa

The cells were assayed for the concentrations of mouse Type I, II and III collagen using an enzyme immunoassay kit (DUMABIO, Shanghai, China) to determine the effect of ligaments and articular cartilage repair in response to the PAs/

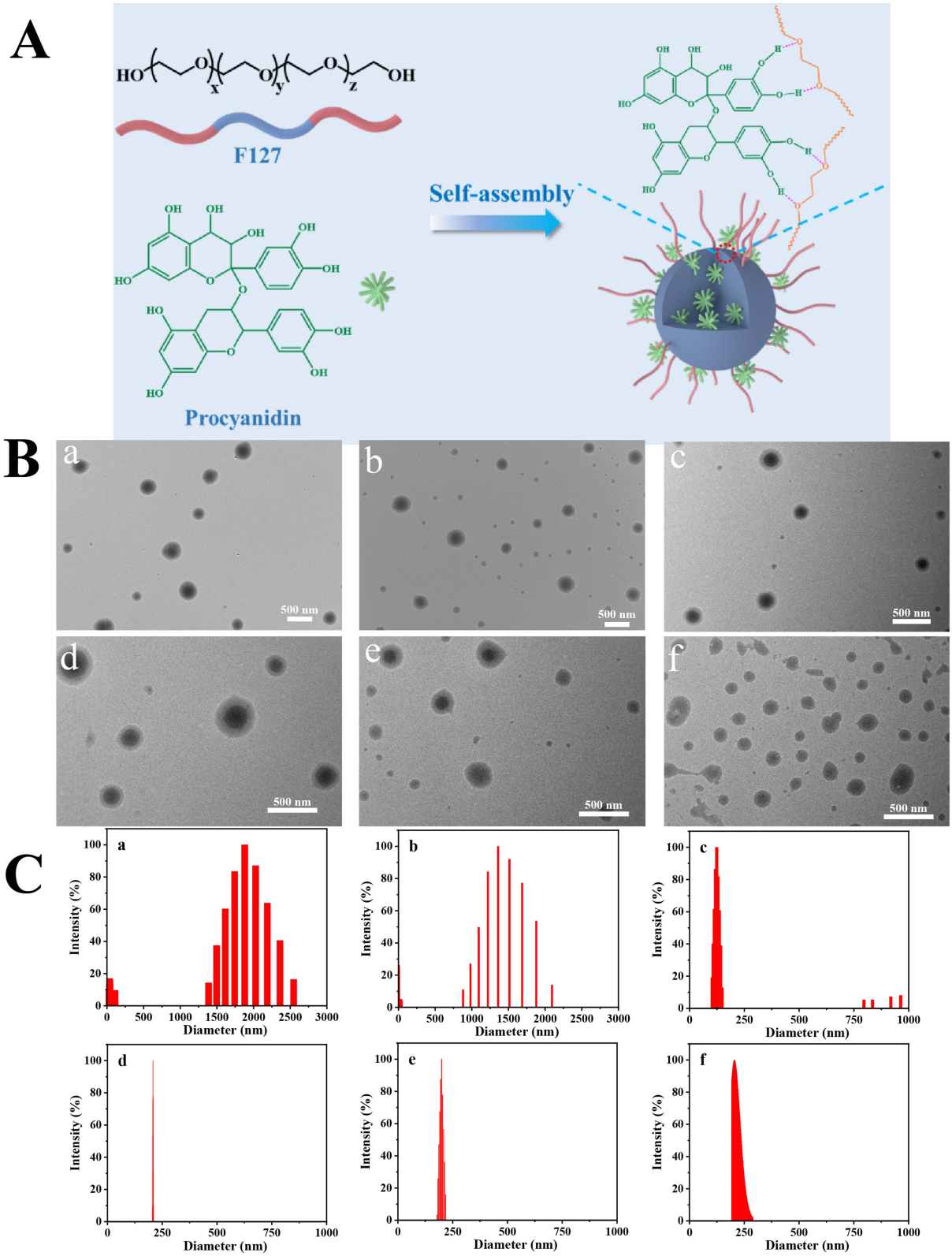

Figure 1 Preparation and characterization of PAs/PF127 nanospheres. (**A**) Schematic illustration of the assembly process of procyanidin-based nanospheres. (**B**) TEM images of (a) PAs-1/PF127, (b) PAs-2/PF127, (c and d) PAs-3/PF127, (e) PAs-4/PF127 and (f) PAs-5/PF127. (**C**) DLS curves of (a) PF127, (b) PAs-1/PF127, (c) PAs-2/PF127, (d) PAs-3/PF127, (e) PAs-4/PF127 and (f) PAs-5/PF127.

Table 1 The Fraction of the PAs/PF127 Nanospheres

	PF127	PAs
PAs-1/PF127	50 mg	10 mg
PAs-2/PF127	50 mg	20 mg
PAs-3/PF127	50 mg	50 mg
PAs-4/PF127	50 mg	75 mg
PAs-5/PF127	50 mg	100 mg

PF127 nanospheres. ELISA kits were utilized as per manufacturer's instructions, and the absorbance was measured by a microplate reader. The amount of collagen was calculated based on the standard curve. Each group contained three parallel holes.

Chondrogenic Differentiation and Alcian Blue Staining

After ADTC5 chondrocytes reached 80% confluence, 0%–20% PAs/PF127-DMEM was supplemented with 10^{-7} M dexamethasone, 120 μM ascorbic acid (Hyclone, Logan, USA), 1% ITS (Sigma-Aldrich, St. Louis, USA), and 10 ng mL^{-1} transforming growth factor-beta 3 (TGF-β3, Cell inspire Bio, Shenzhen, China). The differentiation medium was changed every 2 days. After 14 days of induction differentiation, the glycosaminoglycan synthesis was analyzed with alcian blue staining (Solarbio, Beijing, China). The cultures were washed with DPBS three times and fixed with 4% formaldehyde for 30 min, and then the alcian blue was used to stain the cultures for 30 mins. After three washes, the cells were scanned under a phase contrast microscope. The quantitative method was referred to previous study.[23] Briefly, alcian blue stained cultures were extracted with 6 M guanidine-HCl (Solarbio, Beijing, China) overnight, and the OD was determined at 630 nm. The experiments were performed on triplicates in each group.

In vivo Assays

All animal experimental procedures were approved by the ethical committee of Lanzhou University First Hospital (LDYYLL2024-124), and the animal use protocol followed for the Chinese National Laboratory Animal-Guidelines for Ethical Review of Animal Welfare (GB/T 35892-2018). All animals were supplied from the Lanzhou Veterinary Research Institute of the Chinese Academy of Sciences. Rats were hosted group-cages under the condition of room temperature with free access to clean animal food and drinking water. The in vivo assays were performed using two rats per group.

Six-week-old male Sprague-Dawley rats (SD rat, 180–200g) were used to establish the osteoarthritis model with papain (Solarbio, Beijing, China).[24,25] Briefly, male SD rats (180 g–200 g) were injected with 50 μL 4% papain into double knee-joint on day 1, 4 and 7. After 2 weeks, MRI and hematoxylin and eosin (HE) staining were used to evaluate whether the osteoarthritis model was successfully established. Then, the osteoarthritis SD rats were treated with 50 μL PAs/PF127 nanospheres, PF127 or PAs into the right knee-joint, and an equal volume DPBS was injected into the left knee-joint as a control. The intervention was administered every 10 days. After the 20 days intervention, both knee joints of the osteoarthritis rat were examined by MRI, then the rats were euthanized and knee joints collected for HE staining. Detailed methodology is provided in Supplemental information. All the rats were anesthetized with 10% hydrated chlorine aldehyde, and the method of euthanasia was cervical dislocation.

Statistical Analysis

All data were represented as the mean and standard deviation. SPSS Statistics 27 was used for statistics, and Bonferroni correction was used after ANOVA; p-values for each test was shown in the Supplemental information (Tables S1–S13), and p-values less than 0.05 ($p < 0.05$) were considered indicative of significance.

Result and Discussion

Preparation and Characterization of PAs/PF127

Procyanidin (PAs), as a type of flavonoids, could be extracted from natural plants, and known for their anti-inflammatory and antioxidant properties. Past studies indicated that PAs could reduce cartilage cell apoptosis triggered by IL-1β through inhibit the NF-κB and Nrf2/BAX/Bcl-2 pathway[26,27] and enhance the expression of the cartilage matrix through regulated the expression of pro-inflammatory cytokines.[28–30] These are considered to have a positive effect on the repair process of osteoarthritis (OA). Unfortunately, PAs are an easily degradable drug with poor water solubility, and this would limit the clinical application to a certain extent.

Thus, we designed injectable nanospheres to achieve PAs efficient delivery and release. Figure 1A illustrates the synthetic process of PAs/PF127 assembly nanospheres. A facile self-assembly strategy is used to synthesize the PAs/PF127 nanospheres through the hydrogen bonding between PAs and PF127, as well as the hydrophobic interactions of poly(propylene oxide) chains in PF127. In the assembly process, PF127 is fixed at 50 mg in the total volume of 10 mL DMSO, and the amounts of procyanidin are adjusted to 10, 20, 50, 75, or 100 mg. PAs/PF127 nanospheres are obtained through dialysis in an aqueous solution. The obtained nanospheres are named PAs-n/PF127, where n=1, 2, 3, 4 or 5. As shown in Figure 1B, TEM is used to investigate the morphologies of PAs/PF127 nanospheres. The PAs-1/PF127 exhibits a spherical structure with a large size (Figure 1B(a)). When the procyanidin rises to 20 mg, the PAs-2/PF127 displays a regular spherical structure with a diameter of 250 nm (Figure 1B(b)). The PAs-3/PF127 exhibits a uniform spherical structure with a diameter of 120 nm when the procyanidin rises to 50 mg (Figure 1B(c) and B(d)). On the other hand, PAs-4/PF127 exhibits a regular spherical structure with an increased size of about 140 nm (Figure 1B(e)). Additionally, PAs-5/PF127 exhibits a spherical structure with uneven sizes (Figure 1B(f)). During the assembly process, the hydrophobic interactions between the poly(propylene oxide) chains in PF127 form the inner core of PAs/PF127, while hydrogen bonding between the PEG chains and PA constructs the crown of the nanosphere. As the PA content increases, the crown expands, leading to a gradual decrease in the particle size of the nanospheres, thereby maintaining their stability. Furthermore, when the amount of PAs was increased to 75 mg, a small amount of dark precipitate formed, indicating an excess of PAs, causing instability in the assembled nanospheres. Moreover, dynamic light scattering (DLS) was employed to characterize the hydrodynamic particle sizes of the series of PAs/PF127 nanospheres (Figure 1C). The DLS results confirm a similar trend in particle size variation as observed in TEM analysis. Specifically, the PF127 nanospheres display a wide distribution of micron-sized particles (Figure 1C(a)). With the introduction of PAs, there is an observed decrease in the size of PAs/PF127 nanospheres. The size of PAs-1/PF127 is approximately 1358 nm (Figure 1C(b)), while the size of PAs-2/PF127 is reduced to 208 nm (Figure 1C(c)). Furthermore, PAs-3/PF127 exhibits the smallest particle size at 124 nm (Figure 1C(d)). On the other hand, the size of PAs-4/PF127 increases to 200 nm (Figure 1C(e)), and the size of PAs-5/PF127 increases to 205 nm (Figure 1C(f)) due to the higher amount of procyanidin introduced. Additionally, all PAs/PF127 nanospheres exhibit a typical Tyndall effect (Figure S1). Zeta potential analysis of PAs/PF127 is conducted, and the results are presented in Figure 2A. The series of PAs/PF127 exhibited a negative charge, primarily attributed to the negative charge provided by the phenol hydroxyl group of procyanidin. Consequently, an increase in the procayanidin content led to an increase in the negative charge from −20.2 mV to −42.4 mV. Moreover, PAs-3/PF127 exhibits better dispersion compared to PAs-4/PF127 (Figure S2). Additionally, PAs-3/PF127 has a higher drug content, making it the preferred choice for subsequent experiments.

Fourier transform infrared spectroscopy (FT-IR) spectra of PF127, PAs and PAs/PF127 are presented in Figure 2B. The broad absorption band, peaking at 3377 cm^{-1}, is assigned to the formation of hydrogen bonds between the phenolic hydroxyl groups of procyanidin. The absorption bands at 1611 and 1107 cm^{-1} are attributed to the characteristic functional groups of the polyflavonoid moiety in PAs. The peaks at 1520 and 782 cm^{-1} are ascribed to the skeletal stretching modes of the aromatic ring in the PA structure and the out-of-plane deformation of the aromatic rings with two adjacent free hydrogen atoms. In the PAs/PF127, the characteristic absorption bands are quite similar to PAs, except for stronger hydrogen bonds between the phenolic hydroxyl of procyanidin and the poly(ethylene oxide) chain of PF127 at 3402 cm^{-1}. This indicates that the hydrogen bonding between PAs and PF127 is the driving force for self-assembly.

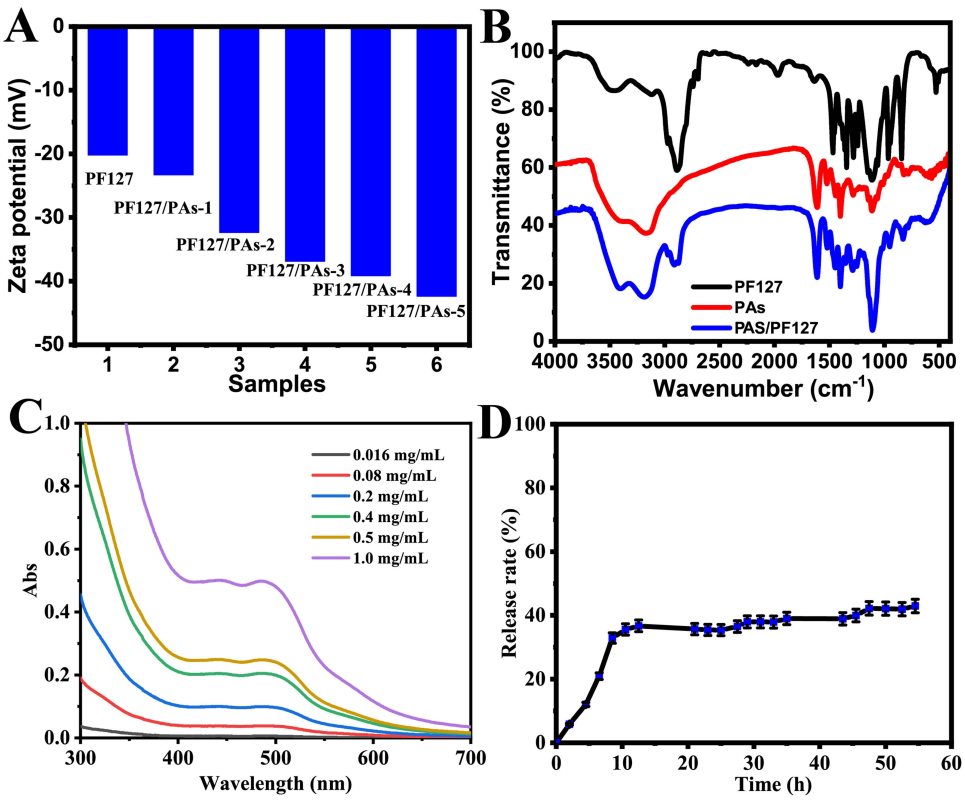

Figure 2 Characterization of PAs/PF127 nanospheres. (**A**) Zeta potential of PAs/PF127 nanospheres. (**B**) FTIR spectrum of PF127, PAs and PAs-4/PF127. (**C**) UV-vis spectra of procyanidin with different concentration. (**D**) In vitro controlled release from the PAs/PF127 in pH 7.4 PBS media.

The PA releasing process of PAs-PF127 nanospheres in vitro was further quantify through UV-visible spectrum under pH 7.4 PBS at 37 °C. As shown in Figure 2C, PAs-PF127 have a characteristic longitudinal absorption peak at 500 nm wavelength, a burst release was detected and the drug release reached plateau after 10 h. The final release rate of PAs was about 42.7% at 57 hours (Figure 2D). Since the complex in vivo environment, the actual PA release might be higher than in vitro results, factors such as the changes in synovial fluid components,[31] viscosity,[32] and friction joint motion may all lead to the degradation of nanospheres and result in the release of PAs. This result confirmed the drug release of PAs-PF127 nanospheres and further indicated the good bioavailability in the joint cavity for the osteoarthritis treatments.

Effects of PAs/PF127 on the Cell Viability in Mouse Fibroblasts and Chondrocytes

The biocompatibility of PAs/PF127 nanospheres was evaluated using CCK-8 assay. OA is primarily caused by the regression of cartilage and ligaments, thus fibroblast L929 cells and chondrogenic cell lines ATDC5 cells were used for in vitro experiments. As shown in Figure 3A(a and b), the viability of both L929 cells and ADTC5 cells in 20% PAs/PF127 groups is significantly lower than other groups after the 4 days intervention. In contrast, the 5–10% PAs/PF127 groups exhibit similar viability to the vehicle, indicating that low concentration of PAs/PF127 nanospheres (≤10%) is nontoxic to chondrocytes and fibroblast. When the same PF127 or PA concentration of 10% PAs/PF127 were performed with CCK-8 assay, the results suggested no significant difference in viability between the PAs/PF127 nanospheres and PF127 (Figure 3A(a and b) box). Interestingly, the same concentration of PA results in inferior viability. This is not surprising since PAs are cytotoxic at certain concentrations.[33] However, after the encapsulation of PF127, the viability was greatly increased, possibly due to the non-cytotoxic nature of PF127 and the retarded release of cytotoxic PAs. To visualize the biocompatibility of PAs/PF127 nanospheres, a Live & Dead Staining was performed. As shown in Figure 3B, strong green fluorescence signals are observed in the PF127 and 5%–10% PAs/PF127. However, when the concentration of PAs/PF127 increases to 20%, the green fluorescence signal intensity decreases significantly in both cell lines, and red fluorescence appears. A similar phenomenon occurs in PA groups (same concentration as 10% PAs/PF127).

https://doi.org/10.2147/IJN.S496827

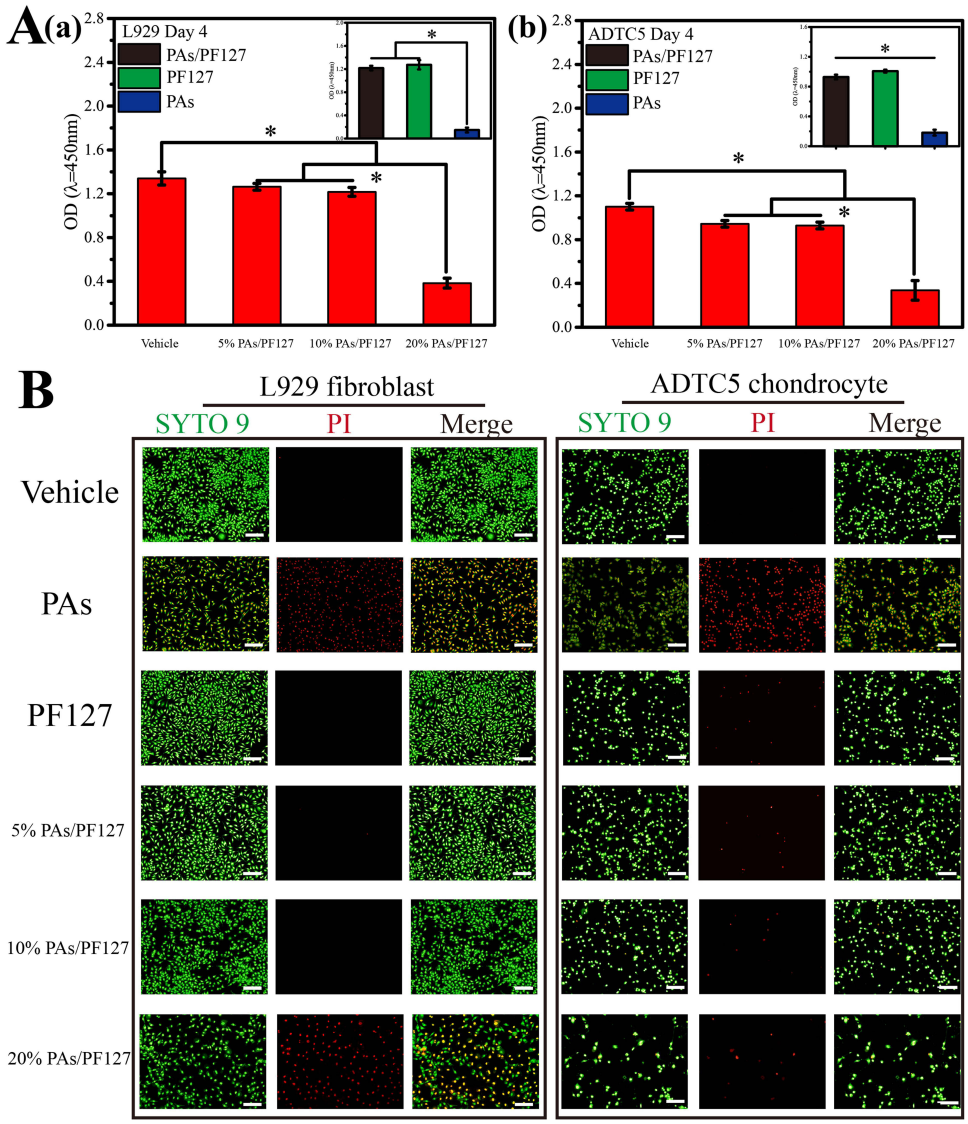

Figure 3 Biocompatibility of mouse L929 fibroblasts and ADTC5 chondrocytes after treated with PAs/PF127. (**A**) Cell viability of L929 cells (a) and ADTC5 cells (b) after co-culturing with PAs/PF127 for 4 days. (**B**) Live (green)/dead (red) staining was used to confirm the biocompatibility of PAs/PF127 nanospheres. Bar=50 μm, and *p < 0.05.

These results confirm that the encapsulation of PF127 significantly reduces cell death and cytotoxicity caused by PAs, further supporting the good biocompatibility of low concentrations PAs/PF127 nanospheres.

Effects of PAs/PF127 on the Expression of Collagen and Glycosaminoglycan in Cells

The potential application of repairing ligaments and cartilage in vitro was systematically assessed by measuring the expression of collagen and glycosaminoglycan. COL1A1 and COL3A1 are major structural protein of bone and ligaments.[34,35] The Elisa kit is used to evaluate and quantitatively analyze the collagen secretion of L929 fibroblast after being treated with PAs/PF127 nanospheres. As shown in Figure 4a, the expression of COL1A1 and COL3A1 significantly increases with increasing concentrations of PAs/PF127. However, this trend quickly reverses when the concentration of PAs/PF127 reaches to 20%. This result suggests that PAs/PF127 promotes the expression of COL1A1 and COL3A1 in L929 fibroblasts at low concentrations but inhibits at high concentrations. This may be attributed to the drug activity of the loaded PAs, as the intervention of PAs significantly increases collagen expression (same concentration as 10% PAs/PF127, subfigure 4Aa, Ab). Pre-experiment results also show that the PAs (0–0.01 mg/mL) can significantly enhance the expression of COL1A1, further confirming the bioactivity of PAs (Figure S3). Although the COL3A1 expression of L929 fibroblasts seems increased, these differences were not statistically significant (Figure S3). Previous research has confirmed the bioactivity effects of PAs, which involve several signaling pathways, such as

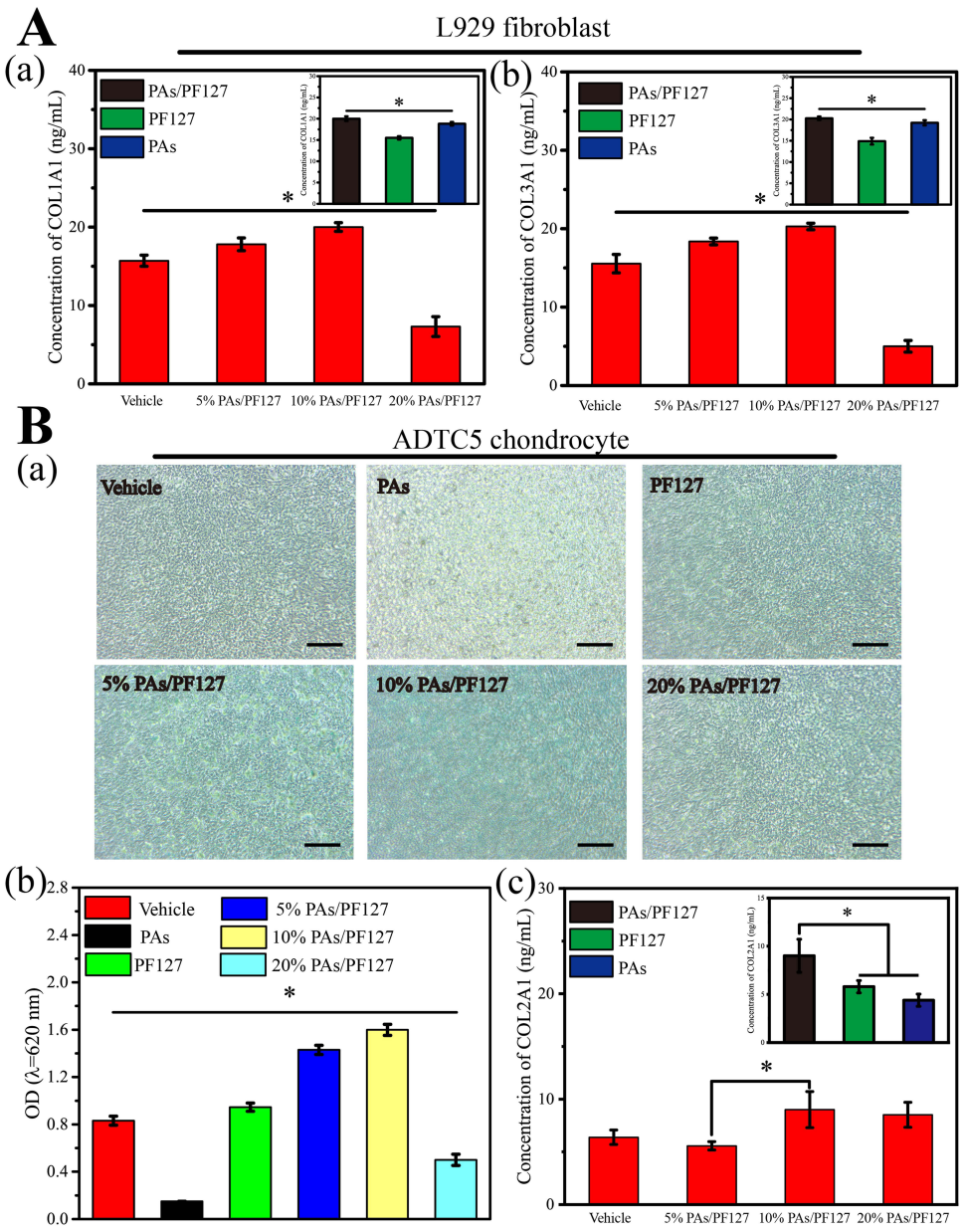

Figure 4 The treatment of PAs/PF127 nanospheres changed the core protein expression patterns of L929 fibroblast and ADTC5 chondrocyte in vitro. (**A**) PAs/PF127 nanospheres enhanced the COL1A1(a) and COL3A1(b) expression of L929 fibroblast after 14 days' co-culture. (**B**) PAs/PF127 nanospheres enhanced the glycosaminoglycan (a, b) and COL2A1(c) expression of ADTC5 chondrocytes after 14 days' co-culture. Bar=100 μm, and * $p < 0.05$.

MAPK, PI3K/Akt/mTOR and NF-κB signaling pathway.[36–38] These pathways participate in the modulation of collagen expression and accelerate fibrogenesis. Moreover, the expression of COL2A1 and glycosaminoglycan in ADTC5 chondrocytes was quantified to evaluate the cartilage repair biofunction of PAs/PF127. Glycosaminoglycan expression was evaluated using alcian blue staining. The PA-only group shows light staining after the 14 days intervention, possibly due to the drug's cytotoxicity. However, after encapsulation with PF127, the staining progressively turns blue with the increasing concentration of PAs/PF127 nanoparticle. Quantitative results further reinforce this conclusion (Figure 4B(a and b)). However, too high concentration of PAs/PF127 represents flare-responsive drug release, which may be responsible for the low glycosaminoglycan expression when the PAs/PF127 concentration research 20%.

In addition, with the increasing concentrations of PAs/PF127, the expression of COL2A1 displayed increasing trends, and statistical differences revealed between 5% PAs/PF127 and 10% PAs/PF127 (Figure 4B(c)). Compared with PAs group and PF127 group, 10% PAs/PF127 significantly promoted the expression of COL2A1, this result may be attributed

https://doi.org/10.2147/IJN.S496827

to the controlled PAs release by PAs/PF127. These results indicate that PAs/PF127 nanospheres can significantly enhance the expression of collagen and glycosaminoglycan in cells, which is considered significant in the treatment of OA.[39,40]

In vivo Assay

To investigate the effect of PAs/PF127 nanospheres on OA, papain was injected into the SD rat knee joint to establish an in vivo animal model.[41] As shown in Figure 5A, two weeks after the modeling, the resting layer and proliferative layer are severely destructed by enzymatic hydrolysis. The morphology of the hypertrophic chondrocytes also significantly

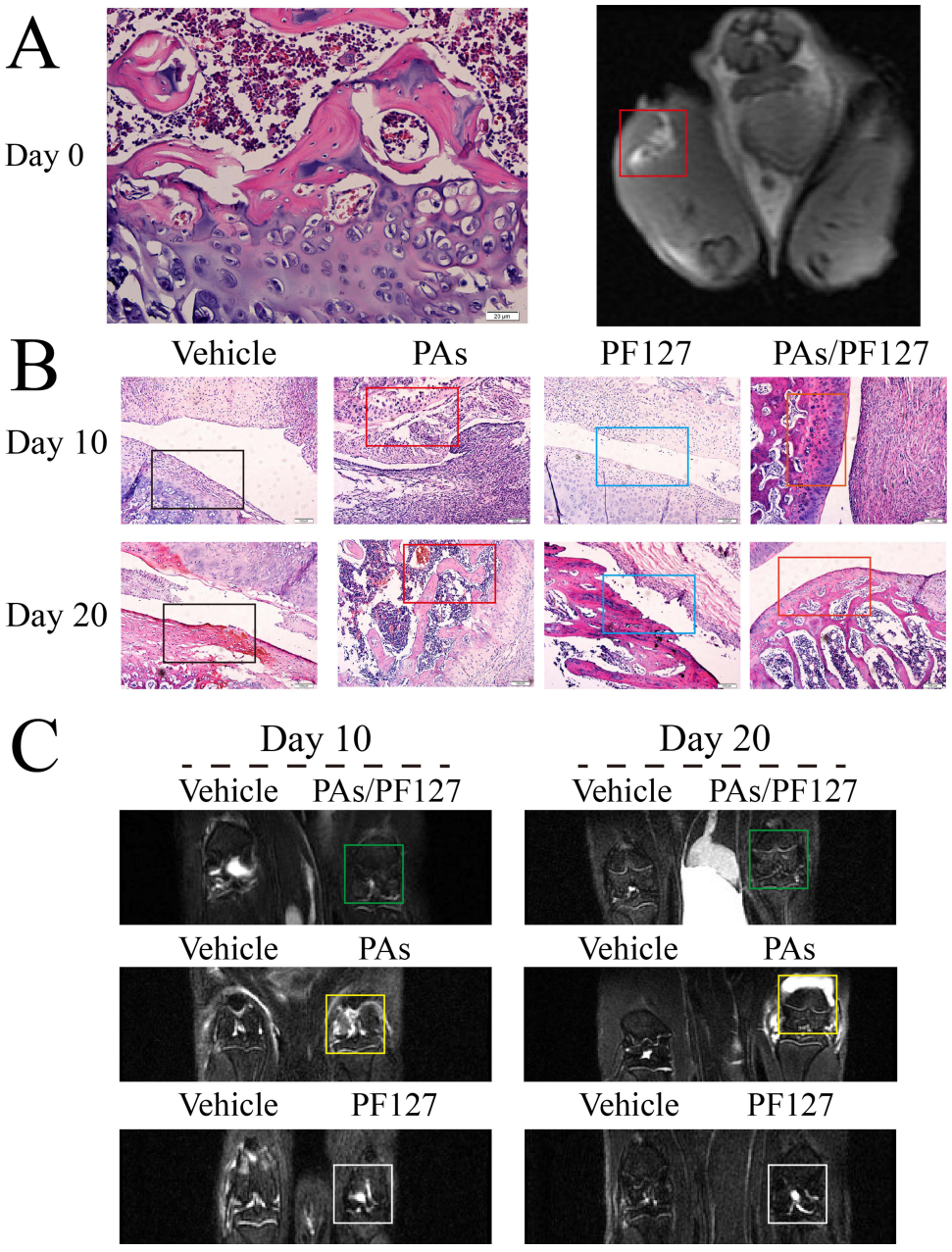

Figure 5 The joint cavity injection of the PAs/PF127 nanospheres in vivo, and the ability for the OA treatment was further evaluated by H&E staining and MRI. (**A**) Establish rat OA model using papain. To Determine the validity of the model, the left leg was considered as the experimental leg and the right leg as the vehicle. The changes of chondrocytes morphology and left knee joint cavity effusion (red box) indicated the effectiveness of OA model. (**B**) The H&E staining of the rat knee joints on the 10 and 20 days indicated that PAs/PF127 nanospheres could excellently repair the OA and achieve cartilage construct repair. Black box: Rough cartilage surface with inflammatory cell infiltration. Red box: Dramatic inflammatory cell infiltration, and insoluble PA agglomerate mass persist. Blue box: Inflammatory cells noticeably decreased. Orange box: Intact cartilage construct repair, and active subchondral bone formation. (**C**) The MRI images of the rat knee joint on the 10 and 20 days indicated that PAs/PF127 nanospheres could reduce joint swelling. Green box: The knee joint with swelling reduced. Yellow box: The single PAs exacerbated knee joint swelling responses. White box: The joint swelling did not show significant improvement. Bar=20 μm.

changes under papain intervened. MRI images show joint cavity effusion after induction of the model (Figure 5A, red box), but not in the contralateral side. These results confirm the effectiveness of the disease models (Figure 5B); then, both legs were modeled as OA (Figure 5B). For the vehicle group, the enzymatic joints are consistently destroyed with inflammatory cell infiltration, and the cartilage surface is rough or even partially lost (Figure 5B, Black box). The intervention of PAs significantly exacerbates inflammatory cell infiltration, and insoluble PA agglomerate mass persists, damaging cartilage through drug toxicity and friction force. Despite this, active bone formation is observed after PA treatment (Figure 5B, Red box). A single PF127 treatment improves OA to some extent. Specifically, the inflammatory cell infiltration is reduced (Figure 5B, Blue box), possibly thanks to the lubricating effect of PF127.[42] Unlike other groups, PAs/PF127 can excellently repair the OA to the normal status. There is no evident inflammatory cell infiltration in the early stage, and new bone formation is greatly enhanced while achieving cartilage construct repair (Figure 5B, Orange box). The reason may be that the PAs/PF127 achieve slow release of PAs. PAs have strong biological activity for antioxidant, anticancer, anti-inflammatory and antibacterial functions, attributed to their ability to scavenge free radicals and inhibit lipid peroxidation.[43,44] Our experimental results also show that the addition of PAs helps improves the expression of collagen and glycosaminoglycan, indicating that PAs have great potential for application in tissue engineering materials of bone, cartilage and skin. Coronal MRI also show that the immediate use of PAs led to soft tissue swelling around the joint, which may be due to the inflammatory response caused by burst release of PAs (Figure 5C, yellow box). After a single PF127 treatment, the joint did not appear to relieve the edema (Figure 5C, white box). Treatment with PAs/PF127 nanospheres reduces joint swelling at early stages, which is quite important for pain control and accelerated healing (Figure 5C, green box).

Conclusions

In conclusion, we have developed an injectable, biocompatibility and self-assembling PA nanospheres (PAs/PF127), made of a self-assembly strategy based on PF127 and PAs through the hydrogen-bond interaction. PAs/PF127 nanospheres have shown promising results in enhancing cell viability and promoting collagen and glycosaminoglycan production in mouse L929 fibroblasts and ADTC5 chondrocytes because of the PA release. Nevertheless, some limitations are also inevitable in this study. Uncertainty exists over the self-assembly strategy because of the sensitivity to the surrounding environment, this might lead to the variability between different batch. Complex synovial fluid microenvironment in osteoarthritis have also limited the quantification of bioavailability in vivo. Despite these limitations, these nanospheres have demonstrated significant potential in reducing joint space swelling and accelerating cartilage healing in an enzymolysis model of rat OA. This work provides a valuable strategy for cartilage healing and OA repairing.

Acknowledgments

This research is supported by grants from the Gansu Provincial Party Committee Organization Department 2021 Longyuan Youth Innovation and Entrepreneurship Talent Project (21LQTD26), the 2023 Fund application conversion project of the first hospital of Lanzhou University (ldyyyn 2023-75), and the Natural Science Foundation of Gansu Province (24JRRA1080).

Funding

(1) Gansu Provincial Party Committee Organization Department 2021 Longyuan Youth Innovation and Entrepreneurship Talent Project (21LQTD26). (2) The 2023 Fund application conversion project of the First Hospital of Lanzhou University (ldyyyn 2023-75). (3) Natural Science Foundation of Gansu Province (24JRRA1080). (4) National Natural Science Foundation of China (11925204).

Disclosure

The authors declare no competing financial interest.

References

1. Wieland HA, Michaelis M, Kirschbaum BJ, Rudolphi KA. Osteoarthritis-an untreatable disease? *Nat Rev Drug Discov*. 2005;4(4):331–344. doi:10.1038/nrd1693
2. Richard MJ, Driban JB, McAlindon TE. Pharmaceutical treatment of osteoarthritis. *Osteoarthr Cartilage*. 2023;31(4):458–466. doi:10.1016/j.joca.2022.11.005
3. Song Y, Zhang J, Xu H, et al. Mesenchymal stem cells in knee osteoarthritis treatment: a systematic review and meta-analysis. *J Orthop Transl*. 2020;24:121–130. doi:10.1016/j.jot.2020.03.015
4. Liu Q, Niu J, Li H, et al. Knee Symptomatic Osteoarthritis, Walking Disability, NSAIDs Use and All-cause Mortality: population-based Wuchuan Osteoarthritis Study. *Sci Rep*. 2017;7(1):3309. doi:10.1038/s41598-017-03110-3
5. Deng S, Zhou JL, Peng H, Fang HS, Liu F, Weng JQ. Local intra-articular injection of vascular endothelial growth factor accelerates articular cartilage degeneration in rat osteoarthritis model. *Mol Med Rep*. 2018;17(5):6311–6318. doi:10.3892/mmr.2018.8652
6. Kawata K, Koga H, Tsuji K, et al. Extracellular vesicles derived from mesenchymal stromal cells mediate endogenous cell growth and migration via the CXCL5 and CXCL6/CXCR2 axes and repair menisci. *Stem Cell Res Ther*. 2021;12(1):414. doi:10.1186/s13287-021-02481-9
7. Migliore A, Paoletta M, Moretti A, Liguori S, Iolascon G. The perspectives of intra-articular therapy in the management of osteoarthritis. *Expert Opin Drug Deliv*. 2020;17(9):1213–1226. doi:10.1080/17425247.2020.1783234
8. Rychel JK. Diagnosis and Treatment of Osteoarthritis. *Top Companion Animal Med*. 2010;25(1):20–25. doi:10.1053/j.tcam.2009.10.005
9. Vinikoor T, Dzidotor GK, Le TT, et al. Injectable and biodegradable piezoelectric hydrogel for osteoarthritis treatment. *Nat Commun*. 2023;14(1):6257. doi:10.1038/s41467-023-41594-y
10. Kang ML, Im G-I. Drug delivery systems for intra-articular treatment of osteoarthritis. *Expert Opin Drug Deliv*. 2014;11(2):269–282. doi:10.1517/17425247.2014.867325
11. Nelson AE. Osteoarthritis year in review 2017: clinical. *Osteoarthr Cartilage*. 2018;26(3):319–325. doi:10.1016/j.joca.2017.11.014
12. Stone S, Malanga GA, Tjpp C. Corticosteroids: review of the history, the effectiveness, and adverse effects in the treatment of joint pain. *Pain Physician*. 2021;24(S1):S233.
13. He Z, Wang B, Hu C, Zhao J. An overview of hydrogel-based intra-articular drug delivery for the treatment of osteoarthritis. *Colloid Surf B*. 2017;154:33–39. doi:10.1016/j.colsurfb.2017.03.003
14. Lei L, Cong R, Ni Y, et al. Dual-Functional Injectable Hydrogel for Osteoarthritis Treatments. *Adv Healthc Mater*. 2024;13(5):2302551. doi:10.1002/adhm.202302551
15. Barbucci R, Lamponi S, Borzacchiello A, et al. Hyaluronic acid hydrogel in the treatment of osteoarthritis. *Biomaterials*. 2002;23(23):4503–4513. doi:10.1016/S0142-9612(02)00194-1
16. Petit A, Sandker M, Müller B, et al. Release behavior and intra-articular biocompatibility of celecoxib-loaded acetyl-capped PCLA-PEG-PCLA thermogels. *Biomaterials*. 2014;35(27):7919–7928. doi:10.1016/j.biomaterials.2014.05.064
17. Wang QS, Xu BX, Fan KJ, Fan YS, Teng H, Wang TY. Dexamethasone-loaded thermo-sensitive hydrogel attenuates osteoarthritis by protecting cartilage and providing effective pain relief. *Ann Transl Med*. 2021;9(14):1120. doi:10.21037/atm-21-684
18. Leong DJ, Choudhury M, Hanstein R, et al. Green tea polyphenol treatment is chondroprotective, anti-inflammatory and palliative in a mouse posttraumatic osteoarthritis model. *Arthritis Res Ther*. 2014;16(6):508. doi:10.1186/s13075-014-0508-y
19. Yao DD, Yang L, Wang Y, et al. Geniposide promotes beta-cell regeneration and survival through regulating β-catenin/TCF7L2 pathway. *Cell Death Dis*. 2015;6(5):e1746–e1746. doi:10.1038/cddis.2015.107
20. Deligiannidou G-E, Papadopoulos R-E, Kontogiorgis C, Detsi A, Bezirtzoglou E, Constantinides T. Unraveling Natural Products' Role in Osteoarthritis Management-An Overview. *Antioxidants*. 2020;9(4):348. doi:10.3390/antiox9040348
21. An X, Zhou F, Li G, et al. Cyaonoside A-loaded composite hydrogel microspheres to treat osteoarthritis by relieving chondrocyte inflammation. *J Mater Chem B*. 2024;12(17):4148–4161. doi:10.1039/D4TB00294F
22. Su J, Yu M, Wang H, Wei Y. Natural anti-inflammatory products for osteoarthritis: from molecular mechanism to drug delivery systems and clinical trials. *Phytother Res*. 2023;37(10):4321–4352. doi:10.1002/ptr.7935
23. Newton PT, Staines KA, Spevak L, et al. Chondrogenic ATDC5 cells: an optimised model for rapid and physiological matrix mineralisation. *Int J Mol Med*. 2012;30(5):1187–1193. doi:10.3892/ijmm.2012.1114
24. Lu Y, Zhang CY, Jiang SL, Yuan F. Anti-Dlx5 Retards the Progression of Osteoarthritis through Inhibiting Chondrocyte Hypertrophy and Apoptosis. Article. *Evid-Based Complement Altern Med*. 2022;6:5019920. doi:10.1155/2022/5019920
25. Ou CP, Chen PF, Song JQ, et al. Alleviation of Papain-Induced Osteoarthritis by Recombinant Human Endostatin via Downregulation of Matrix Metalloproteinase-13, Interleukin-1 and Interleukin-6 in Rats. *J Biomater Tissue Eng*. 2022;12(3):625–629. doi:10.1166/jbt.2022.2893
26. Cai W, Zhang Y, Jin W, et al. Procyanidin B2 ameliorates the progression of osteoarthritis: an in vitro and in vivo study. *Int Immunopharmacol*. 2022;113:109336. doi:10.1016/j.intimp.2022.109336
27. Govoni M, Danesi F. Do Pomegranate Hydrolyzable Tannins and Their Derived Metabolites Provide Relief in Osteoarthritis? Findings from a Scoping Review. *Molecules*. 2022;27(3):1033. doi:10.3390/molecules27031033
28. Li H, Xiang D, Gong C, Wang X, Liu L. Naturally derived injectable hydrogels with ROS-scavenging property to protect transplanted stem cell bioactivity for osteoarthritic cartilage repair. *Original Research Front Bioeng Biotech*. 2023;10:1109074. doi:10.3389/fbioe.2022.1109074
29. Miller MJS, Bobrowski P, Shukla M, Gupta K, Haqqi TM. Chondroprotective effects of a proanthocyanidin rich Amazonian genonutrient reflects direct inhibition of matrix metalloproteinases and upregulation of IGF-1 production by human chondrocytes. *J Inflamm*. 2007;4(1):16. doi:10.1186/1476-9255-4-16
30. Haslauer CM, Elsaid KA, Fleming BC, Proffen BL, Johnson VM, Murray MM. Loss of extracellular matrix from articular cartilage is mediated by the synovium and ligament after anterior cruciate ligament injury. *Osteoarthr Cartilage*. 2013;21(12):1950–1957. doi:10.1016/j.joca.2013.09.003
31. Guelfi M, Fabbrini R, Guelfi MG. Intra-articular treatment of knee and ankle osteoarthritis with polynucleotides: prospective case record cohort vs historical controls. *J Biol Regul Homeost Agents*. 2020;34(5):1949–1953. doi:10.23812/20-238-l
32. Gerwin N, Hops C, Lucke A. Intraarticular drug delivery in osteoarthritis. *Adv Drug Delivery Rev*. 2006;58(2):226–242. doi:10.1016/j.addr.2006.01.018

33. Chen J, Chen Y, Zheng Y, Zhao J, Yu H, Zhu J. Relationship between Neuroprotective Effects and Structure of Procyanidins. *Molecules*. 2022;27(7):2308. doi:10.3390/molecules27072308
34. Swinnen FKR, Coucke PJ, De Paepe AM, et al. Osteogenesis imperfecta: the audiological phenotype lacks correlation with the genotype. *Orphanet J Rare Dis*. 2011;6(1):88. doi:10.1186/1750-1172-6-88
35. Smith LB, Hadoke PWF, Dyer E, et al. Haploinsufficiency of the murine Col3a1 locus causes aortic dissection: a novel model of the vascular type of Ehlers–Danlos syndrome. *Cardiovasc Res*. 2010;90(1):182–190. doi:10.1093/cvr/cvq356
36. Shen H, Han J, Liu C, Cao F, Huang Y. Grape Seed Proanthocyanidins Exert a Radioprotective Effect on the Testes and Intestines Through Antioxidant Effects and Inhibition of MAPK Signal Pathways. *Original Research Front Med*. 2022;8:836528. doi:10.3389/fmed.2021.836528
37. Chen L, You Q, Hu L, et al. The Antioxidant Procyanidin Reduces Reactive Oxygen Species Signaling in Macrophages and Ameliorates Experimental Colitis in Mice. *Original Res Front Immunol*. 2018;8:1910. doi:10.3389/fimmu.2017.01910
38. Nie C, Zhou J, Qin X, et al. Reduction of apoptosis by proanthocyanidin-induced autophagy in the human gastric cancer cell line MGC-803. *Oncol Rep*. 2016;35(2):649–658. doi:10.3892/or.2015.4419
39. Laurens E, Schneider E, Winalski CS, Calabro A. A synthetic cartilage extracellular matrix model: hyaluronan and collagen hydrogel relaxivity, impact of macromolecular concentration on dGEMRIC. *Skeletal Radiol*. 2012;41(2):209–217. doi:10.1007/s00256-011-1331-z
40. Zhu C, Han S, Zeng X, Zhu C, Pu Y, Sun Y. Multifunctional thermo-sensitive hydrogel for modulating the microenvironment in Osteoarthritis by polarizing macrophages and scavenging RONS. *J Nanobiotechnol*. 2022;20(1):221. doi:10.1186/s12951-022-01422-9
41. Lv G, Wang B, Li L, et al. Exosomes from dysfunctional chondrocytes affect osteoarthritis in Sprague-Dawley rats through FTO-dependent regulation of PIK3R5 mRNA stability. *Bone Joint Res*. 2022;11(9):652–668. doi:10.1302/2046-3758.119.Bjr-2021-0443.R2
42. Lei Y, Wang Y, Shen J, et al. Injectable hydrogel microspheres with self-renewable hydration layers alleviate osteoarthritis. *Sci Adv*. 2022;8(5):eabl6449. doi:10.1126/sciadv.abl6449
43. Elejalde E, Villarán MC, Alonso RM. Grape polyphenols supplementation for exercise-induced oxidative stress. *J Int Soc Sport Nutr*. 2021;18(1):3. doi:10.1186/s12970-020-00395-0
44. Cory H, Passarelli S, Szeto J, Tamez M, Mattei J. The Role of Polyphenols in Human Health and Food Systems: a Mini-Review. *Mini Review Front Nutr*. 2018;5:370438. doi:10.3389/fnut.2018.00087